Figure 6. Three day of the temporal variation of TEC values 19 - 21 April 2020, G1 Geomagnetic storm on April 20, as comparison of TEC measurement of GIM-IGS TEC (black dash line), GOPI-GPSTEC (blue line), IRI2016 (thin black dash line) and GoTEC-LAPAN (red line)

Development of a Regional Ionospheric TEC Map for Indonesia

Asnawi Husin[1]*, Buldan Muslim[1], Rizal Suryana[1], Volvariella Volvacea[1], Dyah RM[1], Agung Setyawan[2]

[1]Space Science Center , National Institute of Aeronautic and Space, LAPAN

[2]Geospatial Information Agency , Badan Informasi Geospasial (BIG)

*Correspondence: asnawi@lapan.go.id ; Tel.:+62 226012602

Background

- It is well known that ionosphere has significantly influences radio propagation to distant places on the Earth
- In order to monitor and understand the physics that control the dynamics of the ionosphere, a number of global and regional ionospheric model and data mapping product have been developed over the last several decades.
- The models and data mapping products can provide information regarding change in the ionosphere on a daily basis, hourly basis, or near real time.
- The most ionospheric map are based on total electron content (TEC). The TEC data map are developed based on observations from hundreds of Global Navigation Satellite System (GNSS) receivers.
- The magnitude of TEC varies from a few total electron content unit, 1 TECU = 10^{16} el m^{-2} (TECU) near the magnetic equator to 20–50 TECU at the crest region depending on the day and season [Bagiya et al ., 2009].
- TEC observations from ground-based GPS/ GNSS receivers are often uneven in distributions and concentrated over specific areas because of limited numbers of satellites and stations.
- An interpolation methods have an important role to play in develop ionospheric data mapping product, even on a regional scale.
- Previously reported interpolation technique for TEC-mapping studies include kriging, cubic B-spline and multiquadric (Stanislawska et al 2002., Wielgosz et al 2003., Orùs et al 2005., Grynyshyna-Poliuga et al 2014), as well as moving average covered area (Takahashi et al., 2016). Other technique based on least squares collocation (Krypiak-Gregorczyk et al., 2017) and Spherical cap harmonic (Liu et al 2010) have also been reported.
- In this paper, an ionospheric TEC mapping product (GoTEC-LAPAN) is developed based on multi-GNSS (GPS and GLONASS) observations for the Indonesian region. Method and performance of the ionospheric TEC mapping are carefully analyzed and validated using single station observation data and global model. The TEC data mapping product will be provided in a standard IONEX format so that it can be used for GNSS position correction application purpose.

Objectives

- ✓ To developed ionospheric TEC mapping product (GoTEC-LAPAN) based on multi-GNSS (GPS and GLONASS) observations for the Indonesian region
- ✓ To validated by using single station observation data and global model. The TEC data mapping product will be provided in a standard IONEX format so that it can be used for GNSS position correction application purpose

Data and Method

Figure 1 : Indonesian Continuously Operating Reference Station by ***Badan Informasi Geospasial*** (BIG): http://nrtk.big.go.id/sbc/

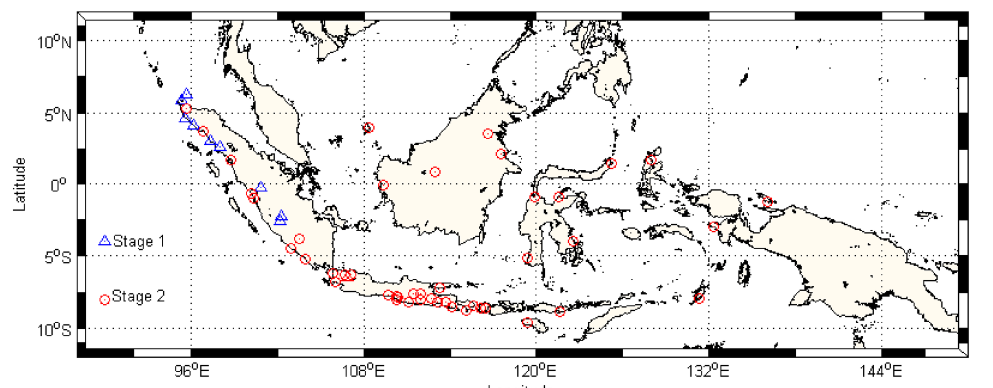

Figure 2 : Geographical map marking the locations of ground-baed GNSS receiver stations from the INACORS BIG network that listed in table 1

Table 1. Geographic coordinate ground GNSS network station INA in this study

No	Station Code	Geographic Latitude	Geographic Longitude
1	CSAB	5.893	95.316
2	CBDA	5.296	95.609
3	CLAN	4.635	95.577
4	CBOH	4.135	96.129
5	CKTF	3.086	97.333
6	CSBS	2.643	98.001
7	CSEL	-0.201	100.839
8	CAGM	-2.56	102.194
9	CBKL	-2.203	102.266
10	CBPI	3.74	96.839
11	CTGR	-6.291	106.664
12	CRAU	2.149	117.497
13	CJKT	-6.11	106.884
14	CTUL	-8.066	111.906
15	CBTU	-6.308	107.096
16	CNGA	-7.605	111.905
17	CMLG	-7.98	112.663
18	CSIB	1.741	98.776
19	CSAU	-7.984	131.298
20	CKRI	-5.196	103.931
21	CBDA	5.296	95.609
22	CNAU	3.586	116.621
23	CLHT	-3.795	103.533
24	CPDG	-0.954	100.363
25	CPUT	0.877	112.923
26	CNAT	3.941	108.388
27	CSMP	-7.196	113.252
28	CBIT	1.443	125.187
29	CNDE	-8.842	121.651
30	CAMP	-0.871	121.579
31	CBIK	-1.186	136.09
32	CFAK	-2.924	132.304
33	CPON	-0.004	109.329
34	CKEN	-3.963	122.545
35	CMAK	-5.135	119.408
36	PALP	-0.916	119.906
37	CPTS	-8.009	110.302
38	CPAR	-0.625	100.132
39	CPES	-8.534	114.11
40	CTBL	1.73	128.008
41	CANA	-4.446	102.924
42	CPDG	-0.954	100.363
43	CKBM	-7.67	109.653
44	CMAG	-7.606	111.451
45	CTUL	-8.066	111.906
46	CBTL	-7.893	110.336
47	JOGS	-7.817	110.295
48	CPAC	-8.196	111.098
49	CMLG	-7.98	112.663
50	CLUM	-8.214	113.115
51	CELO	-8.621	116.471
52	CJEM	-8.175	113.693
53	CDNP	-8.818	115.146
54	CBAG	-8.441	115.613
55	CMAT	-8.583	116.098
56	CKRI	-5.196	103.931
57	CPSR	-6.226	105.834
58	CBAK	-9.638	119.409
69	CMLP	-6.778	106.019
70	BAKO*	-6.49	106.852
71	NTUS*	1.34	103.67
72	BDNG**	-6.5	107.3

In the first step, we subtract P1, P2,,L1, L2 and ECEF location antenna data from RTCM streaming via NTRIP. The slant TEC values derived from pseudorange measurement $STEC_P$ and carrier phase measurements $STEC_\Phi$ (Liu 2004) as following formula:

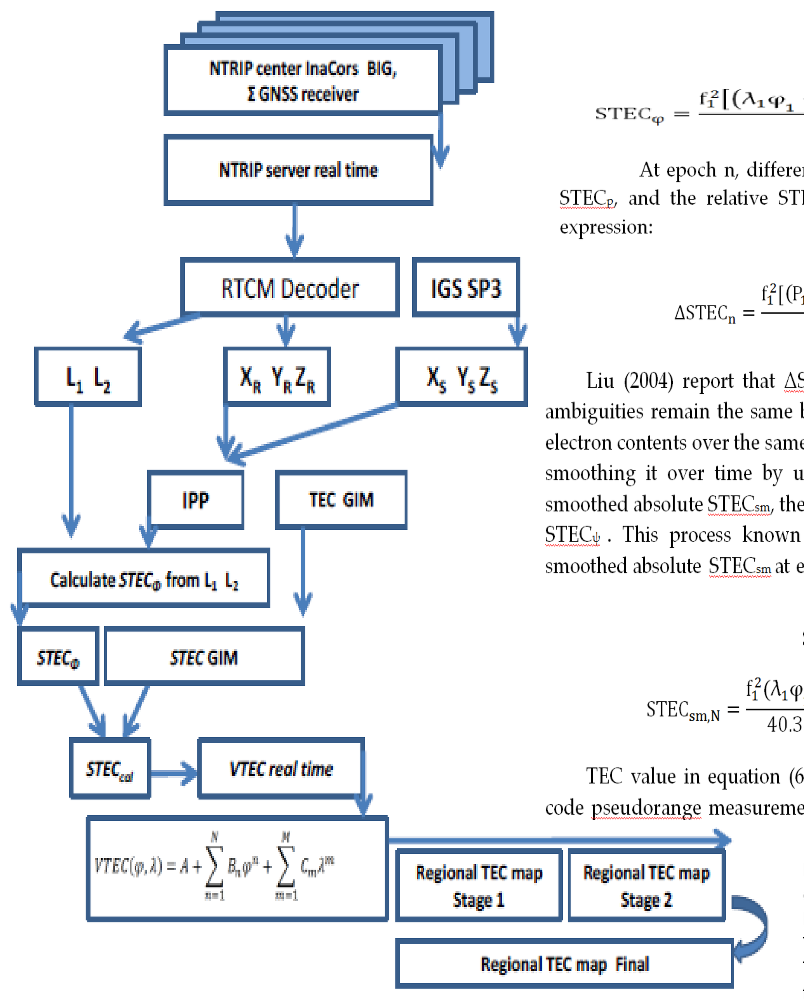

$$STEC_p = \frac{f_1^2[(P_1 - P_2) - b_p - B_p}{40.3(1-\gamma)} \quad (1)$$

$$STEC_\varphi = \frac{f_1^2[(\lambda_1\varphi_1 - \lambda_2\varphi_2) - (\lambda_1 N_1 - \lambda_2 N_2) - b_\varphi - B_\varphi]}{40.3(1-\gamma)} \quad (2)$$

At epoch n, differencing equations (1) and (2) results in an offset between the absolute $STEC_P$, and the relative $STEC_\Phi$ which is denoted as $\Delta STEC_n$ with the following mathematical expression:

$$\Delta STEC_n = \frac{f_1^2[(P_1 - P_2) - b_p - B_p + (\lambda_1\varphi_1 - \lambda_2\varphi_2}{40.3(1-\gamma)} + \frac{f_1^2[-(\lambda_1 N_1 - \lambda_2 N_2) - b_\varphi - B_\varphi}{40.3(1-\gamma)} \quad (4)$$

Liu (2004) report that $\Delta STEC_n$ have constant value over time as long as the carrier phase ambiguities remain the same because both $STEC_P$ and $STEC_\psi$ are measurements of the same total electron contents over the same location and at the same time. The precise ΔSTEC can be obtained by smoothing it over time by using the recursive equation (Skone, 1998). In order to obtain the smoothed absolute $STEC_{sm}$, the offset between absolute and relative TEC can be added to the relative $STEC_\psi$. This process known as carrier phase leveled code pseudorange TEC derivation. The smoothed absolute $STEC_{sm}$ at epoch N is expressed as:

$$STEC_{sm,N} = STEC_{\varphi N} + \Delta STEC_N \quad (5)$$

$$STEC_{sm,N} = \frac{f_1^2(\lambda_1\varphi_1 - \lambda_2\varphi_2)}{40.3(1-\gamma)} + \frac{1}{N}\sum_{n=1}^{N}\left(\frac{f_1^2[(P_1 - P_2) + (\lambda_1\varphi_1 - \lambda_2\varphi_2)]}{40.3(1-\gamma)}\right) + \frac{f_1^2(-b_p - B_p)}{40.3(1-\gamma)} \quad (6)$$

TEC value in equation (6) still containing the satellite and receiver inter-frequency biases on code pseudorange measurements b_P and B_P that can be estimated within the ionospheric model.

However in this study we calibrated $STEC_{sm}$ in equation (6) using the differential code bias (DCB) data provided by Center for Orbit Determination in Europe (CODE) at ftp://ftp.unibe.ch/aiub/CODE/. The third step is convert slant TEC ($STEC_{sm}$) into vertical TEC (VTEC). The VTEC obtained by multiplying the STEC with the mapping function M(z), which, is defined as:

$$(STEC_{sm,R}^{S})_N = M(z)(VTEC_{sm,R}^{S})_N \quad (7)$$

with

$$M(z) = \left[1 - \left(\frac{R_e}{R_e + h}\right)^2 \sin^2 z\right]^{1/2} \quad (8)$$

In the last step (4), the goal is to provide vertical TEC maps (grids). In order to do so we used VTEC spatial variation using second order polynomial function for latitudinal variation and first order polynomial function for longitudinal variation. The polynomial TEC function of latitude (Φ) and longitude (λ) as follow:

$$VTEC(\varphi, \lambda) = A + \sum_{n=1}^{N} B_n\varphi^n + \sum_{m=1}^{M} C_m\lambda^m \quad (9)$$

Finally in order to see deviation and comparison with global model, GoTEC-LAPAN is evaluated based on Mean Absolute Percentage Error (MAPE).

$$MAPE = \frac{100\ \%}{n}\sum_{1}^{n}\left|\frac{R-G}{R}\right| \quad (10)$$

with

Φ = Ionospheric Pierce Point (IPP) latitude

λ = IPP longitude

N = order of polynomial functions for TEC variations with respect to latitude = 2

M = order of polynomial functions for TEC variations with respect to longitude = 1

Results and Discussion

To test and validation our method, IGS global ionospheric model (GIM), IRI2016 and single-station observation data during a geomagnetic storm event were used to evaluate the TEC map model. The solar storm happened on April 20, Figure 4 shows the variations of the geomagnetic parameters, (Bz, Kp and Dst) from April 19 to 21, 2020. These indices can be obtained from NASA's OMNI website (https://omniweb.gsfc.nasa.gov/form/dx1.html). The situation shown in figure 4 indicates that the North South component of interplanetary magnetic field (IMF-Bz) jumped to -14nT, Kp 5 and Dst index reached about -60 nT, (started at 06:00 UT), which was categorized as minor G1 geomagnetic storm conditions.

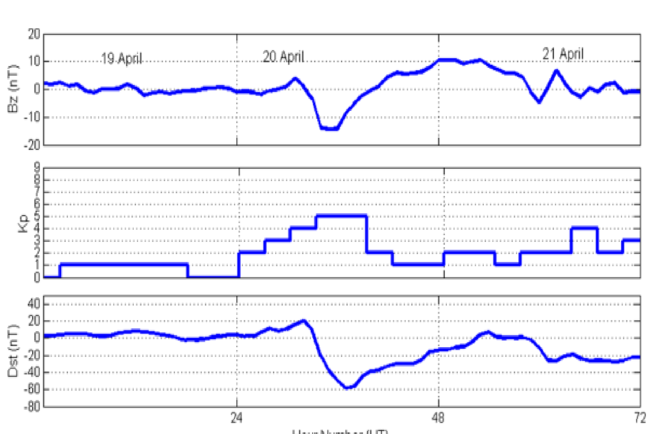

Figure 4. Interplanetary and geomagnetic indexes from April 19 to 21, 2020 (a) The interplanetary magnetic field BZ component (nT), (b) Kp index , (c) Dst index (nT)

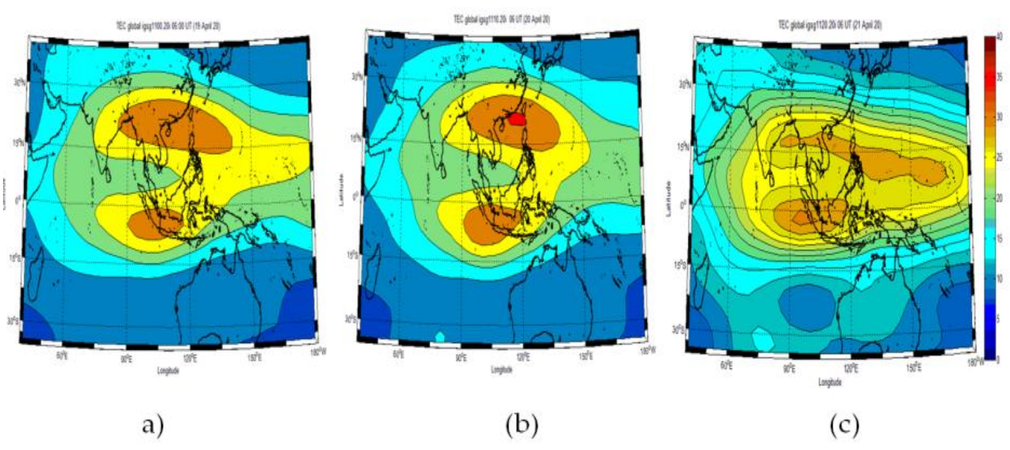

Figure 5. Three day of the global TEC values for Asia region obtained from GIMs produced by the IGS a) 19 April, b) 20 April, G1 geomagnetic storm day and c) 21 April 2020

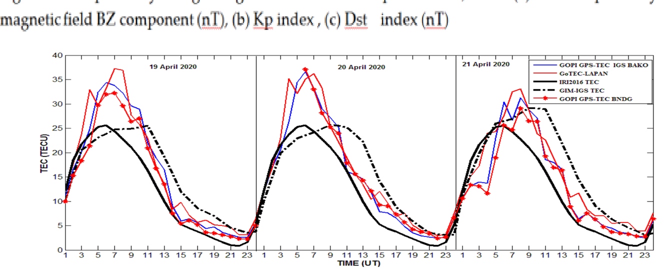

Figure 6. Three day of the temporal variation of TEC values 19 - 21 April 2020, G1 Geomagnetic storm on April 20, as comparison of TEC measurement of GIM-IGS TEC (black dash line), GOPI-GPSTEC (blue line), IRI2016 (thin black dash line) and GoTEC-LAPAN (red line)

The results in Figure 6 show three days of temporal variations of TEC for model and observations. These include GIM-IGS TEC (black dash line), Gopi-GPSTEC at BAKO (blue line), IRI2016 (thin black dash line) and GoTEC-LAPAN (red line). We can see that the global TEC model, (IRI2016 and GIM-IGS TEC) are lower than regional model (GoTEC-LAPAN) and single-station observation data (Gopi-GPSTEC at BAKO). The TEC values from GoTEC-LAPAN and Gopi-GPSTEC at BAKO have have a similar pattern.

.Apparently, the minor geomagnetic storm did not significantly affect the expected regular TEC variation. This might be because both set of measurements ware taken in the southern crest region (SCR), while the effect of TEC asymmetries during this geomantic storm primarily affected the northern crest region (NCR) as shown in Figure 5.

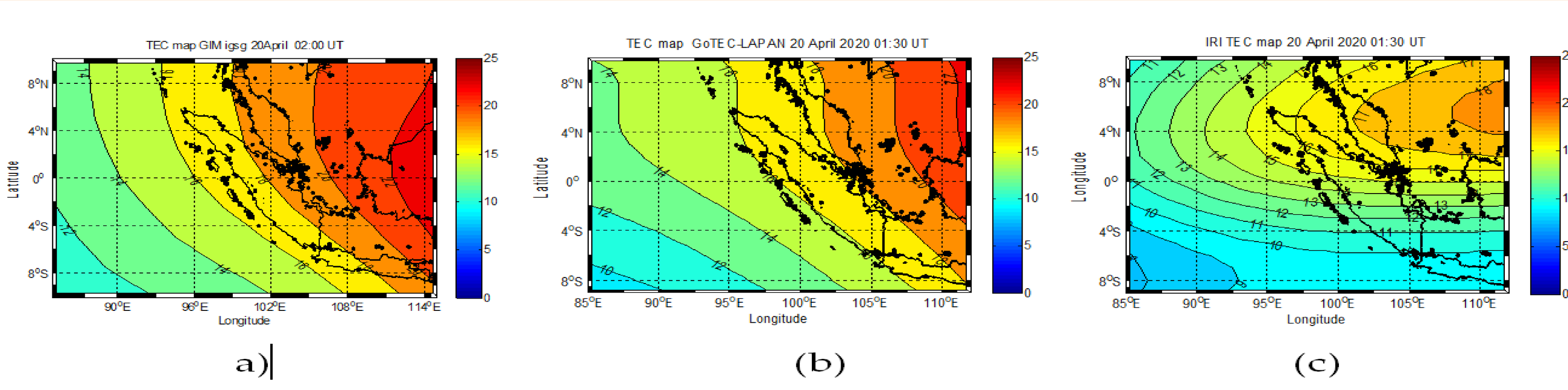

Figure 7. Global TEC (GIM) igs (a), regional TEC GoTEC-LAPAN (b) and IRI2016 TEC model (c) during G1 minor geomagnetic storm on April 20, 2020 by using 10 stations

In the first stage of GoTEC-LAPAN model development, the first 9 GNSS station from INACORS BIG listed in table 1 and indicated as blue triangle in Figure 2, used for developed TEC map of GoTEC-LAPAN model which is covered latitude between 10° North to 10° South and Longitude form 85° to 120°. The TEC map is (marked as blue triangles in Figure 2) were used to developed the TEC map, which covered latitude range between 10°N and 10°S and longitude range from 85°E and 120°E. The TEC map covered the area of Sumatra, Peninsular Malaysia, Java and West Kalimantan. Figure 7 shows a comparison of the global TEC (GIM) IGS (Figure 7(a), TEC IRI2016-TEC (Figure 7(c) model and GoTEC-LAPAN (Figure 7 (b) at 01:30 April 20, 2020. In Figure 7, IGS-GIM TEC and GoTEC-LAPAN model show similar spatial pattern of TEC variation and absolute TEC level, but IRI2016 TEC values were somewhat lower and exhibit different spatial variation. This different is likely due to the use of satellite bias in the TEC estimation method of TEC GIM and GoTEC-LAPAN.

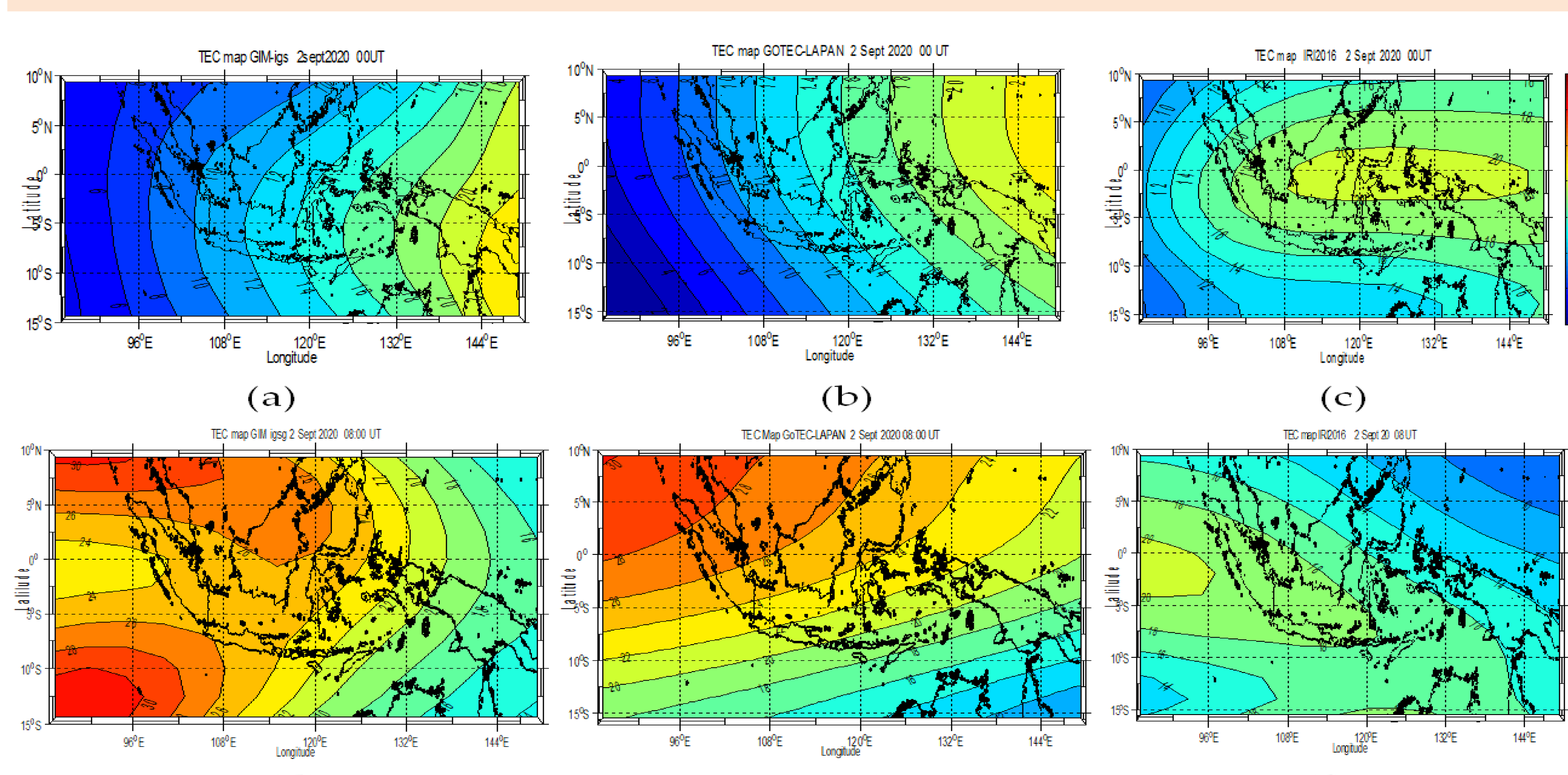

Figure 8. Three ionospheric TEC map model, Global TEC (GIM) igs, regional TEC of GoTEC-LAPAN and IRI2016 TEC model on September 2, 2020 by using 60 stations. a),b) and c) at 00:00 UT, d), e) and f) at 08:00 UT respectively.

Generally, we had developed simple low order polynomial model for TEC mapping over Indonesian sector. Earlier results from stage 1 GoTEC-LAPAN (using 10 GNSS INACORS station, covered latitude range between 10°N and 10°S and longitude range from 85°E and 120°E as shown in Figure 7) showed quite good agreemment IGS-GIM and IRI2016. However, when GoTEC-LAPAN is further expanded by using 60 GNSS station from INACORS (covered latitude range of 10° N to -15°S and longitude range of 85°E to 150°E)), the model results became quite different on spatial patern, especially during day time. Obviously IGS-GIM showed two maximum peak of TEC as a representation of equatorial anomaly (EIA) but GoTEC-LAPAN showed only one peak. The Mean Absolute Percentage Error (MAPE) of GoTEC-LAPAN model respect to IGS-GIM TEC about 14.62 %, and IRI2016 about 32.01%. The IGS-GIM TEC is support by world-wide network of IGS stations, the grids having IGS stations inside would give better accuracy than the grids without any IGS stations. Recently, there are about 5 sites of IGS station in the regional Indonesia, incluing of NTUS Singapore, that makes it even more accurate. However, IGS-GIM has a temporal resolution of two hours and a spatial resolution 2.5° and 5° so it is problem in practical purposes that requiring a resolution of less than two hours. GoTEC-LAPAN is developed by quite simple method of first order polynomial for build regional TEC map. Considering algorithm runtime, the method was choosen to provide near real time of TEC map with temporal resolution 5 minutes and spatial resolution 1° x 1°. However, the next step for the effectiveness of the methods already used, the IONEX format as output of GoTEC-LAPAN need to be testing of accuracy for practical purposes as ionospheric correction model

Conclusion

The regional ionospheric model from the INACORS BIG GNSS network over Indonesia has been developed. The Networked Transport of RTCM via Internet Protocol (NTRIP) used to retrieved RCTM data. TEC values derived from carrier phase measurements and we use satellite and receiver bias from IGS-GIM IONEX data. In the first stage we use 9 sites from INACORS then continued add to be 60 sites in the stage two. Result showed when using 9 site of GNSS INACORS, the IGS-GIM TEC and GoTEC-LAPAN model somewhat the same spatial pattern of TEC variation in the west region Indonesia and agree with TEC value, but IRI2016 TEC values lowest and showing slightly different spatial pattern of TEC variation. This different is due to the use of satellite bias in the TEC estimation method of TEC GIM and GoTEC-LAPAN. In the stage two, model is expanded by using 60 stations of GNSS INACORS, the TEC variation between GoTEC-LAPAN and IGS-GIM TEC quite same spatial patern compared to IRI2016 at 00:00 UT (07:00 LT). However, the model showing quite different of spatial pattern at 08:00 UT (15:00 LT). IGS-GIM TEC showing two highest TEC peak (representation of EIA) compare to GoTEC-LAPAN which is only showing one highest TEC peak. The Mean Absolute Percentage Error (MAPE) of GoTEC-LAPAN model respect to IGS-GIM TEC about 14.62 %, and IRI2016 about 32.01%.

Acknowledgments

We would like to thank Rezy Pradipta for his comments and insightful suggestions of the manuscript. We would like to thank the Indonesian Geospatial Information Agency (Badan Informasi Geospasial–BIG) for the INACORS RTCM data, the International GNSS Service (IGS), ftp://cddis.nasa.gov/gnss/products/ ionex, IRI2016 model https://ccmc.gsfc.nasa.gov/modelweb/models/ iri2016_vitmo.php) for model data and NASA's official website (https://omniweb.gsfc.nasa.gov/form/ dx1.htm, geomagnetic index used in this study..

References

Fejer, B.G. Equatorial Ionospheric Electric Fields Associated With Magnetospheric Disturbances. *Solar wind-Magnetosphere coupling, (Eds) Kamide, Y. and Slavin, J. A., Terra Scientific Publishing Company (TERRAPUB), Tokyo* **1986**, 519–545.

Fejer, B.G. Low Latitude Electrodynamic Drifts: A Review. *Journal of Atmospheric and Terrestrial Physics* **1991**, *53*, 677–693.

Fejer, B. G.; de Paula, E. R.; Gonzales, S. A.; Woodman, R. F. Average vertical and zonal F-region plasma drifts over Jicamarca, *J. Geophys. Res* **1991**, 96, 13 901–13 906.

Fejer, B. G.; Kelley,M. C. Ionospheric irregularities, Rev. *Geophys. Space Phys* **1980**, 18, 401–454.

Bailey, G. J.; Balan, N.; Su, Y. Z. The Sheffield University plasmasphere ionosphere model - a review. *J. Atmos. Terr. Phys* **1997**,59, 1541–1552.

Balan, N.; Bailey, G. J. Equatorial plasma fountain and its effects: Possibility of an additional layer, *J. Geophys. Resv* **1995**, 100, 21 421–21 432.

Balan, N.; Bailey, G. J.; Abdu, M. A.; Oyama, K. I.; Richards, P. G.; MacDougall, J.; Batista, I. S. Equatorial plasma fountain and its effects over three locations: Evidence for an additional layer, the F3-layer, *J. Geophys. Res* **1997**,102, 2047–2056.

Shim, JA Soon. Analysis of Total Electron Content (TEC) Variations in the Low- and Middle-Latitude Ionosphere. (2009). All Graduate Theses and Dissertations. 403. https://digitalcommons.usu.edu/etd/403

Reddybattula, K.D.; Panda, S.K. Performance analysis of quiet and disturbed time ionospheric TEC responses from GPS-based observations, IGS-GIM, IRI-2016 and SPIM/IRI-Plas 2017 models over the low latitude Indian region, *Advances in Space Research* **2019,** 64 (10), pp. 2026-2045.

Tsagouri I.; Koutroumbas, K.; Elias, P. A new short-term forecasting model for the total electron content storm time disturbances. *J. Space Weather Space Clim* **2018**. 8: A33

Bergeot N.; Tsagouri, I.; Bruyninx, C.; Legrand, J.; Chevalier, J. The influence of space weather on ionospheric total electron content during the 23rd solar cycle. *J. Space Weather Space Clim* **2013**, 3, A25.

Grynyshyna-Poliuga, O.; Stanislawska, I.; Swiatek, A. Regional Ionosphere Mapping with Kriging and B-spline Methods. In Mitigation of Ionospheric Threats to GNSS: an Appraisal of the Scientific and Technological Outputs of the TRANSMIT Project **2014**. https://doi.org/10.5772/58776

Bagiya, M. S.; Joshi, H. P.; Iyer, K. N.; Aggarwal, M.; Ravindran, S.; Pathan, B. M. TEC variations during low solar activity period (2005–2007) near the Equatorial Ionospheric Anomaly Crest region in India, *Ann. Geophys* **2009,** 27, 1047– 1057.

Takahashi, H.; Wrasse; C. M.; Denardini, C. M.; Pádua, M. B.; Paula, E. R.; Costa, S. M. A.; Otsuka, Y.; Shiokawa, K.; Monico,J.F.G.I.A.; Sant'Anna, N. IonosphericTEC Weather Map Over South America, *Space Weather*, **2016**,14, 937–949,doi:10.1002/2016SW001474

Stanislawska, I.; Juchnikowski, G.; Cander, L.R.; Ciraolo, L.; Bradley, P.A.; Zbyszynski, Z.; Swiatek, A. The kriging method of TEC instantaneous mapping. *Adv. Space Res* **2002**, 29, 945–948.

Wielgosz, P.; Grejner-Brzezinska, D.A.; Kashani, I. Regional ionosphere mapping with kriging and multiquadric methods. *J. Glob. Position. Syst* **2003**, 2, 48–55.

Orùs, R.; Hernández-Pajares, M.; Juan, J.M.; Sanz, J. Improvement of global ionospheric VTEC maps by using kriging interpolation technique. *J. Atmos. Sol. Terr. Phys* **2005**, 67, 1598–1609.

Krypiak-Gregorczyk, A.; Wielgosz, P.; Jarmołowski, W. A new TEC interpolation method based on the least squares collocation for high accuracy regional ionospheric maps. *Meas. Sci. Technol* **2017**, 28, 045801.

Liu, J., Chen, R., Wang, Z.; Zhang, H. Spherical cap harmonic model for mapping and predicting regional TEC. *GPS Solutions* **2010**, 15,2, 109–119. doi:10.1007/s10291-010-0174-8

Rama Rao, P. V. S.; Gopi Krishna, S.; Niranjan, K.; Prasad, D. S. V. V. D. Temporal and spatial variations in TEC using simultaneous measurements from the Indian GPS network of receivers during the low solar activity period of 2004-2005, *Ann. Geophys* **2006**, 24, 3279-3292, doi:10.5194/angeo-24-3279-2006.

Rajesh, P. K.; Liu, J. Y.; Balan, N.; Lin, C. H.; Sun, Y. Y.; Pulinets, S. A. Morphology of midlatitude electron density enhancement using total electron content measurements, *J. Geophys. Res.- Space Phys* **2016** 1503–1507, https://doi.org/10.1002/2015JA022251.

Dashora, N.; Suresh, S.; & Niranjan, K. Interhemispheric asymmetry in response of low-latitude ionosphere to perturbation electric fields in the main phase of geomagnetic storms. *J. Geophys. Res.- Space Phys* **2019**, 124, 7256– 7282. https://doi.org/10.1029/2019JA026671

Shi, C.,; Zhang, T.; Wang, C.; Wang, Z.; Fan, L. Comparison of IRI-2016 model with IGS VTEC maps during low and high solar activity period. *Results In Physics* **2019,**12,555-561. https://doi.org/10.1016/j.rinp.2018.12.022